doi:10.1038/nature10462

I. A GAP TUNABLE FLUX QUBIT

Superconducting flux-qubits [1, 2], which consist of three Josephson junctions (3JJ) connected by a low inductance superconducting loop, are a promising candidate for constructing quantum processors. The only tunable parameter in this system is the magnetic flux ($\Phi_{\rm m}$) penetrating the loop. At the degeneracy point, namely when $\Phi_{\rm m} = (n+\frac{1}{2})\Phi_0$ (with integer n), the energy spacing between the ground state and first exited state reaches the minimum value "gap (Δ)". The degeneracy point is optimal because at this point the qubit is decoupled from low frequency flux noise and has maximum coherence time [3, 4]. However, the gap of the flux-qubit is untunable since it is only determined by its intrinsic parameters, e.g. Josephson energy E_J and charge energy E_C of the three Josephson junctions. One way to overcome this is to replace the smallest junction of the flux-qubit with a DC-SQUID. By varying the magnetic flux of the DC-SQUID, which is equivalent to changing the parameters of the smallest junction, we can tune the gap of the flux-qubit [5–7]. This is a significant advantage when coupling to other quantum systems. Our flux-qubit can be tuned into or out of resonance with other quantum systems while keeping the qubit at its optimal work point.

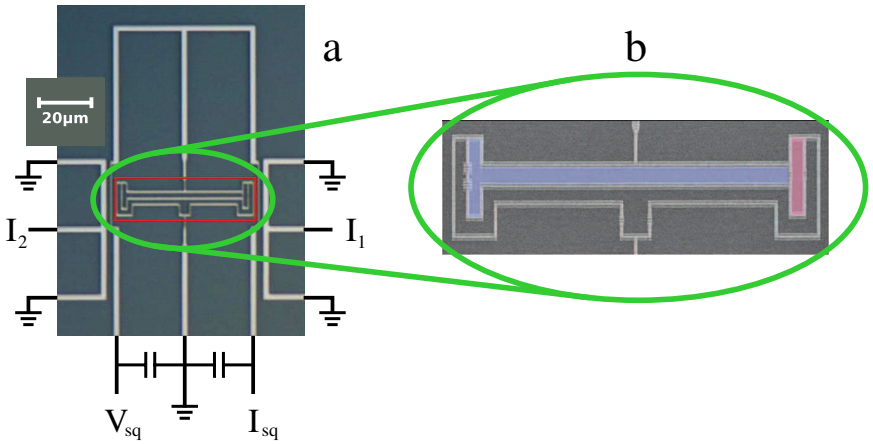

FIG. 1. Optical micrograph and the circuit scheme of the aluminum flux-qubit (a) and a magnified view of the chip under the red box region (b).

Our qubit is shown schematically in Figure 1. The qubit is composed of four Josephson junctions in two loops (Figure 1b); The main loop (blue) and the α control loop (red). The main loop encloses three junctions: two identical junctions with same Josephson energy E_J and one shared with the α control loop with smaller Josephson energy $\alpha_0 E_J$, where α_0 is the ratio of the Josephson energy between the third and first two junctions. The two junctions in the α control loop are identical and form a DC-SQUID. The effective Josephson energy of the DC-SQUID can be tuned by the flux threading the α control loop Φ_α, $\alpha E_J = 2\alpha_0 \cos(\pi\Phi_\alpha/\Phi_0)E_J$. We place two control lines (Figure 1a of the main manuscript) to tune both the effective magnetic flux $\Phi_{\rm m}$ and Φ_α *in situ*. The mutual inductances

* Electronic address: semba.kouichi@lab.ntt.co.jp

between control line 1 with the α control loop and main loop are 90 fH and 256 fH, and those between control line 2 with the α control loop and main loop are 0.5 fH and 549 fH.

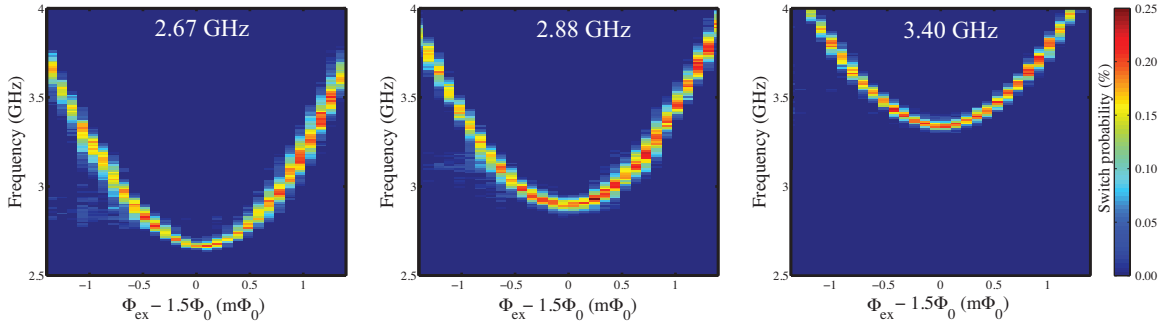

FIG. 2. Spectra with different gaps: (a) 2.67 GHz, (b) 2.88 GHz and (c) 3.40 GHz

We carried out our experiment in the following manner: First we biased Φ_m of the qubit close to $3\Phi_0/2$ by means of the external magnetic coil located in the dewar, then we added the shift pulse via control line 1 and control line 2 to tune Φ_m and Φ_α. The shift of Φ_m caused by control line 1 was compensated with control line 2. Figure 2 shows the spectra with three different gaps. In Figure 2a for example, as the shift pulse voltage level of control line 1 was fixed, we scanned control line 2. As the mutual inductance of control line 2 with the α control loop was much smaller than that with the main loop, we regarded Φ_α (and the gap) as approximately constant during that scan. Therefore, the spectra obtained here are similar to those of the conventional 3JJ flux-qubit. If we want to change the gap of the qubit, we set the shift pulse voltage of control line 1 to another value and scan control line 2. Spectrawere obtained with different gaps (Figure 2b and 2c). Thus by adding the shift pulse of control line 1 and line 2 with different voltages, we can tune the qubit to any working point within these ranges dynamically.

II. VOLUME AND CONCENTRATION ESTIMATION FOR PHOTOLUMINESCENCE MEASUREMENTS

The estimation of the concentration C of NV^- centers in the ensemble is given by $C = P/V$ where P the ratio of the photoluminescence intensities between the ensemble and a single NV^- center, and V the volume of the detected region [8]. The volume is estimated from the confocal scanning image of a single NV^- center (Figure 3a). In the sliced image with respect to the photoluminescence intensity axis (z-axis) and the scanned axis (x-axis), the line shape of the spot of the single NV^- center can be fitted by a Gaussian line shape (Figure 3b). The half width at half maximum of it is estimated to be $193(\pm 2)$ nm. Assuming a column with a radius of 193 nm and height of 500 nm, the volume is approximately $V = 5.85 \times 10^7$ nm^3. With a measured ratio of the intensities $P = 6.45(\pm 0.30) \times 10^4$, the concentration can be estimated as $C = 1.1 \times 10^{18}$ cm^{-3}.

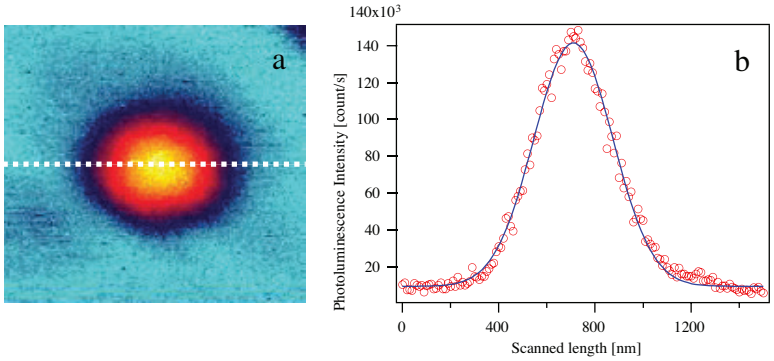

FIG. 3. Confocal microscopy scans of photoluminescence of a single NV^- center (a) and sliced image (b) with respect to photoluminescence intensity axis (z-axis) and the scanned x-axis (shown in (a) as the white dotted line).

III. MODELING OF N NV$^-$ CENTERS COUPLED TO A FLUX QUBIT

The Hamiltonian for our gap tunable flux-qubit coupled to an ensemble of NV$^-$ centers can be represented by

$$H = \underbrace{\frac{h}{2}\left(\Delta\sigma_x + \epsilon\sigma_z\right)}_{H_{\rm F}} + \underbrace{h\sum_i^N \left[DS_{z,i}^2 + E\left(S_{x,i}^2 - S_{y,i}^2\right) + g_{\rm e}\mu_B B_{z,i}S_{z,i}\right]}_{H_{\rm NV}} + \underbrace{\frac{h}{2}\sum_i^N g_i S_{x,i}\sigma_z}_{H_{\rm int}}, \tag{1}$$

where $\sigma_{x,y,z}$ are the usual Pauli operators for the flux-qubit and $S_{x,y,z}$ represent the spin 1 operators of the NV$^-$ centers, $h\Delta$ is the energy of the tunnel splitting, $h\epsilon = 2I_P(\Phi_{\rm ex} - \Phi_0/2)$ is the energy bias, $I_P \approx 300\,{\rm nA}$ is the persistent current in the qubit, $\Phi_{\rm ex}$ is the external flux threading the qubit loop and $\Phi_0 = h/2e$ is the flux quantum. The splitting energy of the gap tunable flux-qubit is $h\sqrt{\epsilon^2+\Delta^2}$, where both ϵ and Δ are controllable by the external magnetic flux threading the two loops. Next D (E) are the zero-field splitting (strain-induced splitting) of a NV$^-$ center ground state with typical values of $D \sim 2.88\,{\rm GHz}$ ($E < 10\,{\rm MHz}$). The term B_zS_z describes the Zeeman interaction of the electronic NV$^-$ spin ($S = 1, g_e = 2.0028, \mu_B = 14\,{\rm MHz}\cdot{\rm mT}^{-1}$). This is negligible in our case as the magnetic field applied perpendicular to the chip surface to prepare the flux qubit is less than 0.1 mT. The coupling (with strength g_i) between the flux-qubit and a NV$^-$ center is given by $\frac{h}{2}g_i\, S_x\sigma_z$.

In line with the experimental parameters, we assume that B and E are small enough to neglect the associated terms in the Hamiltonian (1). After a trivial change of basis on the flux-qubit for simplicity, we get the idealized Hamiltonian

$$H = h\bar{\Delta}\sigma_+\sigma_- + h\sum_i^N \left(DS_{z,i}^2 + \bar{g}_i\sigma_x S_{x,i}\right). \tag{2}$$

where $\bar{g}_i = \frac{g_i}{2}$. Under experimental conditions $\bar{g}_i \ll \bar{\Delta}, D$ and we can make a rotating wave approximation

$$H = h\bar{\Delta}\sigma_+\sigma_- + h\sum_i^N \left(DS_{z,i}^2 + \bar{g}_i\left[\sigma_+\bar{S}_{-,i} + \sigma_-\bar{S}_{+,i}\right]\right), \tag{3}$$

where $\sigma_\pm$ are the usual raising and lower operators for the flux qubit and $\bar{S}_+$ is an *effective* raising operator $\bar{S}_+ = \frac{1}{\sqrt{2}}\left[|1\rangle\langle 0| + |-1\rangle\langle 0|\right]$, not the spin 1 raising operator. We can define collective operators $b = \frac{1}{\sqrt{N}}\sum_i^N \bar{S}_{-,i}$, $b^\dagger = \frac{1}{\sqrt{N}}\sum_i^N \bar{S}_{+,i}$ which allows one to consider the ensemble as a generalized harmonic oscillator strongly coupled to the flux qubit [9, 10].

Under the rotating wave approximation, the Hamiltonian commutes with the number operator $\hat{n} = \sigma_+\sigma_- + \sum_i S_{z,i}^2$ for the system, so that the Hilbert space is limited by the energy at which the system is initialized. If the system is initialized with one excitation then non-dissipative evolution allows access to only $2N+1$ of the possible 2×3^N states of the system, as there are $2N$ possible single excitation states in the N NV$^-$ center ensemble and one of the flux-qubit. The final assumption is that we may model each NV$^-$ center as a qubit, as the energy gap between the $|1\rangle$ and $|-1\rangle$ states is much smaller (nearly degenerate) than the gap between those states and $|0\rangle$. The Hamiltonian used for our model was thus

$$H = h\bar{\Delta}\sigma_{+,\rm F}\sigma_{-,\rm F} + h\sum_i^N \left(DS_{z,i}^2 + \bar{g}_i\left[\sigma_{+,\rm F}\sigma_{-,i} + \sigma_{-,\rm F}\sigma_{+,i}\right]\right), \tag{4}$$

which allows the system with a single excitation to access $N+1$ states. The additional subscript F is to clarify which operators act on the flux-qubit.

The experiment was performed under cryogenic conditions, so that we may assume that the NV$^-$ centers remain in $|0\rangle$ if they are initialized in that state. We modeled the case in which a single excitation is injected into the system via the flux-qubit. For the numerical model we allow a state vector $N+2$ long, due to the addition of the state with no excitations, which will be used to model depopulation. The zeroth (top) entry in the vector is associated with this state. The cryogenic conditions under which the experiment was performed allowed us to assume that the probability of excitations entering the system from the thermal bath was small enough to neglect this process. The next entry is associated with the excited flux qubit, and each of the remaining belongs to one of the N NV$^-$ centers with the excitation. With this order encoded into the state vector, the σ_- and σ_z operators for the flux qubit and first NV$^-$

center are

$$\sigma_{-,\mathrm{F}} = \begin{pmatrix} 0 & 1 & 0 & 0 & \dots \\ 0 & 0 & 0 & 0 & \dots \\ 0 & 0 & 0 & 0 & \dots \\ 0 & 0 & 0 & 0 & \dots \\ \vdots & \vdots & \vdots & \vdots & \ddots \end{pmatrix}, \; \sigma_{z,\mathrm{F}} = \begin{pmatrix} -1 & 0 & 0 & 0 & \dots \\ 0 & 1 & 0 & 0 & \dots \\ 0 & 0 & 0 & 0 & \dots \\ 0 & 0 & 0 & 0 & \dots \\ \vdots & \vdots & \vdots & \vdots & \ddots \end{pmatrix}, \; \sigma_{-,1} = \begin{pmatrix} 0 & 0 & 1 & 0 & \dots \\ 0 & 0 & 0 & 0 & \dots \\ 0 & 0 & 0 & 0 & \dots \\ 0 & 0 & 0 & 0 & \dots \\ \vdots & \vdots & \vdots & \vdots & \ddots \end{pmatrix}, \; \sigma_{z,1} = \begin{pmatrix} -1 & 0 & 0 & 0 & \dots \\ 0 & 0 & 0 & 0 & \dots \\ 0 & 0 & 1 & 0 & \dots \\ 0 & 0 & 0 & 0 & \dots \\ \vdots & \vdots & \vdots & \vdots & \ddots \end{pmatrix}. \quad (5)$$

$\sigma_{-,i}$ is a matrix of zeros with a one in entry $[0, i+1]$ and $\sigma_{z,i}$ is s matrix of zeros with -1 at $[0,0]$ and 1 at $[i+1, i+1]$. Substituting these operators into (4) yields the Hamiltonian

$$H = h \begin{pmatrix} 0 & 0 & 0 & 0 & \dots \\ 0 & \bar{\Delta} & \bar{g}_i & \bar{g}_i & \dots \\ 0 & \bar{g}_i & D & 0 & \dots \\ 0 & \bar{g}_i & 0 & D & \dots \\ \vdots & \vdots & \vdots & \vdots & \ddots \end{pmatrix}. \quad (6)$$

Using these operators we can also generate the decay super-operators associated with T_1 and T_2 for each subsystem. The decay super-operators for depopulation and dephasing for all subsystems are

$$\begin{aligned} L_{\mathrm{F}}^{(1)}[\rho] &= \frac{1}{2T_{\mathrm{F},1}} \left(2\sigma_{-,\mathrm{F}}\rho\sigma_{+,\mathrm{F}} - \sigma_{+,\mathrm{F}}\sigma_{-,\mathrm{F}}\rho - \rho\sigma_{+,\mathrm{F}}\sigma_{-,\mathrm{F}}\right), \\ L_{\mathrm{F}}^{(2)}[\rho] &= \frac{1}{T_{\mathrm{F},2}} \left(\sigma_{z,\mathrm{F}}\rho\sigma_{z,\mathrm{F}} - \rho\right), \\ L_{i}^{(1)}[\rho] &= \frac{1}{2T_{i,1}} \left(2\sigma_{-,i}\rho\sigma_{+,i} - \sigma_{+,i}\sigma_{-,i}\rho - \rho\sigma_{+,i}\sigma_{-,i}\right), \\ L_{i}^{(2)}[\rho] &= \frac{1}{T_{i,2}} \left(\sigma_{z,i}\rho\sigma_{z,i} - \rho\right), \end{aligned} \quad (7)$$

which, together with the Hamiltonian form the Lindblad master equation

$$\frac{\partial\rho}{\partial t} = -i\left[H, \rho\right] + L_{\mathrm{F}}^{(1)}[\rho] + L_{\mathrm{F}}^{(2)}[\rho] + \sum_{i}^{N} \left(L_{i}^{(1)}[\rho] + L_{i}^{(2)}[\rho]\right), \quad (8)$$

where we have assumed zero temperature. This master equation was solved by numerical integration for comparison with the experimental results. The red vacuum Rabi oscillation curve in Figure (4a) of the main manuscript was determined by varying the T_1, T_2 of the flux and diamond subsystem until an agreement was reached.

IV. ESTIMATION OF THE COUPLING STRENGTH FOR A SINGLE NV$^-$ CENTER

As mentioned in Section III, the Hamiltonian for our gap tunable flux qubit coupled to an ensemble of NV$^-$ centers can be represented by (1). We have made several assumptions about the nature of the coupling between the subsystems in this Hamiltonian which we need to justify. The most general coupling term between a single center and the flux-qubit can be written as a weighted summation over all $S_{x,y,z}\sigma_{x,y,z}$ combinations. In our situation the anti-aligned magnetic fields created by the circular persistent current of the flux-qubit are in the z direction and so the dominant coupling terms are of the form $S_{x,y,z}\sigma_z$. Next, our NV$^-$ sample was orientated about the (001) axis where the magnetic field generated by the flux qubit is parallel to the direction of (001) and perpendicular to the crystal surface. This means the $S_z\sigma_z$ is small and can be neglected. This leaves two remaining coupling terms of the form $S_x\sigma_z$ and $S_y\sigma_z$. Our orientation of the NV$^-$ sample means all four possible NV$^-$ spin configurations couple equally to the magnetic field created by the flux qubit. With our high degree of symmetry we can choose the y-axis such that $S_x\sigma_z$ dominates. This means $\frac{h}{2}\sum_i^N g_i S_{x,i}\sigma_z$ is a good representation of the coupling between the flux qubit and the NV$^-$ ensemble in this case [11, 12]. The coupling strength g_i between a flux-qubit and the i^{th} NV$^-$ center spin located above the narrow center region of the qubit main loop can then be roughly estimated as

$$g_i = 2g_{\mathrm{e}}\mu_B B, \quad (9)$$

where the magnetic field B can be estimated using the Biot-Savart law. To first order, $B = \mu_0 I_p/(2R)$. where $\mu_0 = 4\pi \times 10^{-7}\,\mathrm{N}\cdot\mathrm{A}^{-2}$ and R the distance between a flux-qubit and a single NV^- center. In our case it has a typical value of $R \sim 1.2\,\mu\mathrm{m}$. This can be estimated in the following way: The distance from the flux qubit to the center of the flux loop is approximately $0.7\,\mu\mathrm{m}$ and the distance from the center of the flux loop to the center of the diamond ensemble is $0.5\,\mu\mathrm{m}$ (center to diamond surface) + $0.5\,\mu\mathrm{m}$ (diamond surface to ensemble center). Thus the distance from the flux qubit to the center of the ensemble is $\sqrt{0.7^2 + (0.5+0.5)^2} \sim 1.2\,\mu\mathrm{m}$. Given these parameters we can estimate the coupling strength as

$$g_i \sim \frac{g_e \mu_0 \mu_B I_p}{R} \sim 8.8\ \mathrm{kHz}\,. \tag{10}$$

It must be emphasized that this is a very rough estimate. It does not take into account many important effects such as the angular orientation between the color centers (there are four orientations in our case with the same angle with [001] direction to which the magnetic field is generated by the flux-qubit points). However our estimate is consistent with the number of NV^- centers ($N \sim 3.1 \times 10^7$) expected to be directly above the flux qubit.

We can now estimate the effective coupling strength between our flux-qubit and ensemble as $g_{\mathrm{ens}} \sim \sqrt{2N} g_i \sim 70\,\mathrm{MHz}$ (where the factor of 2 is due to the two-fold degeneracy of the excited $|\pm 1\rangle$). The value of $g_{\mathrm{ens}} \sim 70\,\mathrm{MHz}$ is quite interesting as it is much larger than either the decoherence rate of either the flux qubit or the diamond ensemble ($\gamma_{\mathrm{flux-qubit}} \sim 1\,\mathrm{MHz}$, $\gamma_{\mathrm{ensemble}} >\sim 10\,\mathrm{MHz}$). That is $g_{\mathrm{ens}}/\gamma_{\mathrm{flux-qubit}}, g_{\mathrm{ens}}/\gamma_{\mathrm{ensemble}} \gg 1$. We can define a cooperatively parameter $C = g_{\mathrm{ens}}^2/(\gamma_{\mathrm{flux-qubit}}\gamma_{\mathrm{ensemble}}) > 500$. In quantum optical situations, in which an atom is coupled to a cavity, this would be considered strong coupling.

V. COHERENCE TIME OF THE FLUX QUBIT: RAMSEY MEASUREMENTS

It is essential to determine the coherence properties of our flux-qubit with the diamond sample attached to it. To achieve this, we tuned the flux-qubit gap to $\Delta = 3.12\mathrm{GHz}$ ($\sim 240\mathrm{MHz}$ detuned from the NV^- center frequency) and performed Ramsey measurements. The Ramsey measurement sequence starts with a $\pi/2$ RF pulse followed by free evolution for a time τ. After this a second $\pi/2$ RF pulse is applied and the qubit state measured by applying a measurement pulse to the readout SQUID. The frequency of the RF pulse was intentionally detuned from the flux-qubit resonant frequency, so that the Ramsey oscillation could be observed (Figure 4). It can be easily seen from Figure (4a) that the Ramsey decay time reaches a maximum at the degeneracy point ($\Phi_{\mathrm{ex}} = 1.5\Phi_0$). At this degeneracy point (Figure 4b) the coherence time of the flux-qubit is longer than 150 ns. The red curve shown in (4b) is a fit to the experimental data using the model given in Section III.

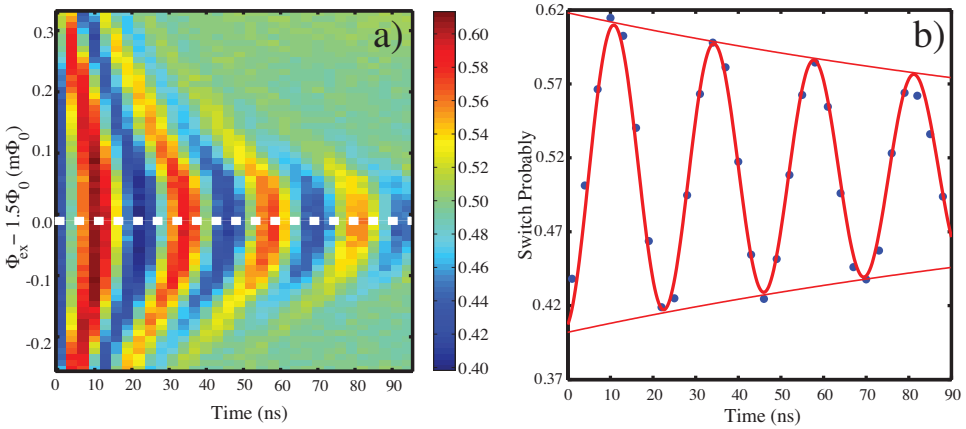

FIG. 4. Ramsey measurements of the flux-qubit - NV^- ensemble coupled system with flux-qubit gap $\Delta = 3.12\,\mathrm{GHz}$. In (a) the switching probability is plotted against $\Phi_{\mathrm{ex}} - 1.5\Phi_0$ and τ the free evolution time. In (b) the switching probability is plotted against τ for $\Phi_{\mathrm{ex}} = 1.5\Phi_0$, corresponding to the white dotted line in (a). It is clearly seen that we have a coherence time in excess of 150 ns.

[1] Mooij, J. E., Orlando, T. P., Levitov, L., Tian, L., van der Wal, C. H. & Lloyd S. Josephson Persistent-Current Qubit. *Science 285*, 1036-1039 (1999).
[2] Orlando, T. P., Mooij, J. E., Tian, L., van der Wal, C. H., Levitov, L. S., Lloyd S. & Mazo, J. J. Superconducting persistent-current qubit, *Phys. Rev.* **B60**, 15398–15413 (1999).
[3] Yoshihara, F., Harrabi, K., Niskanen, A.O., Nakamura, Y. & Tsai. J. S. Decoherence of Flux Qubits due to $1/f$ Flux Noise, *Phys. Rev. Lett.* **97**, 167001 (2006).
[4] Kakuyanagi, K., Meno, T., Saito, S., Nakano, H., Semba. K., Takayanagi, H., Deppe, F. & Shnirman, A. Dephasing of a Superconducting Flux Qubit, *Phys. Rev. Lett.* **98**, 047004 (2007).
[5] Zhu, X., Kemp, A., Saito, S., & Semba, K. Coherent operation of a gap-tunable flux qubit. *Appl. Phys. Lett.* **97**, 102503 (2010).
[6] Paauw, F. G, Fedorov, A., Harmans, C. J. P. M. & Mooij, J. E. Tuning the Gap of a Superconducting Flux Qubit, *Phys. Rev. Lett.* **102**, 090501 (2009).
[7] Fedorov, A., Feofanov, A. K., Macha, P., Forn-Díaz, P., Harmans, C. J. P. M. & Mooij, J. E. Strong Coupling of a Quantum Oscillator to a Flux Qubit at Its Symmetry Point, *Phys. Rev. Lett.* **105**, 060503 (2010).
[8] Mizuochi, N., Neumann, P., Rempp, F., Beck, J., Jacques, V., Siyushev, P., Nakamura, K., Twitchen, D., Watanabe, H., Yamasaki, S., Jelezko & F., Wrachtrup, J. Coherence of single spins coupled to a nuclear spin bath of varying density. *Phys. Rev. B* **80**, 041201(R) (2009).
[9] Kubo, Y., Ong, F. R., Bertet, P., Vion, D., Jacques, V., Zheng, D., Dréau, A., Roch, J.-F., Auffeves, A., Jelezko, F. ,Wrachtrup, J., Barthe, M. F., Bergonzo, P. & Esteve, D. Strong Coupling of a Spin Ensemble to a Superconducting Resonator. *Phys. Rev. Lett.* **105**, 140502 (2010).
[10] Müller, C., Shnirman A. & Makhlin, Y. Relaxation of Josephson qubits due to strong coupling to two-level systems. *Phys. Rev. B* **80**, 134517 (2009).
[11] Marcos, D., Wubs, M., Taylor, J. M., Aguado, R., Lukin, M. D. & Sørensen, A. S. Coupling Nitrogen-Vacancy Centers in Diamond to Superconducting Flux Qubits. *Phys. Rev. Lett.* **105**, 210501 (2010).
[12] Twamley, J. & and Barrett S. D. Superconducting cavity bus for single nitrogen-vacancy defect centers in diamond. *Phys. Rev. B* **81**, 241202(R) (2010).